A MRIEM for Solving the Laplace Equation in the Doubly-Connected Domain

Chein-Shan Liu[1]

Abstract: A new method is developed to solve the Dirichlet problems for the two-dimensional Laplace equation in the doubly-connected domains, namely the *meshless regularized integral equations method* (MRIEM), which consists of three portions: Fourier series expansion, the Fredholm integral equations, and linear equations to determine the unknown boundary conditions on *artificial* circles. The boundary integral equations on artificial circles are singular-free and the kernels are degenerate. When boundary-type methods are inefficient to treat the problems with complicated domains, the new method can be applicable for such problems. The new method by using the Fourier series and the Fourier coefficients can be adopted easily to derive the meshless numerical method. Several numerical examples are tested showing that the new method is powerful.

Keyword: Laplace equation, Meshless method, Regularized integral equation, Artificial circles, Doubly-connected domain, Degenerate kernel

1 Introduction

Numerical methods are required inevitably to solve the engineering problems in complicated domains, since in these situations the analytical solutions are usually not available. Numerical methods used widely are finite difference method (FDM), finite element method (FEM) and boundary element method (BEM). Because the BEM can reduce the dimensionality of the considered problems, it has become an efficient alternative calculational tool to replace the domain-based FDM and FEM. However, there are pitfalls to hamper its efficient implementation. The major

disadvantage of BEM is its singularities: weak singularity of kernel function, Cauchy principal value singularity and hypersingularity.

For a complicated shape of the domain those methods usually require a large number of nodes and elements to match the geometrical shape. In order to overcome these difficulties, Atluri, Kim and Cho (1999) have proposed the meshless local boundary integral equation (LBIE) method, and Atluri and Shen (2002) have proposed the meshless local Petrov-Galerkin (MLPG) method. Both methods use local weak forms, and the integrals can be easily evaluated over regularly shaped domains, like as circles in 2D problems and spheres in 3D problems.

Algorithms based on discretization of integral equations are often attractive for problems with complicated domains because of the reduced complexity of discretization when compared with competive approaches such as FDM and FEM. For this reason there were many researchers devoted to overcome the difficulties arised from the perplexing singularities in the boundary integral equations. At the first, Landweber and Macagno (1969) have proposed method to get rid of the singularity by substracting a function from the integrand so that the kernel becomes non-singular, and then adding back an accurate integration of the function to the integral equation. This method was modified and referred to as the non-singular boundary integral method by Hwang and Hwang (1998) and Fan and Young (2002), or the desingularized boundary integral method by Chuang (1999).

Then, another way to avoid the singularity was proposed by Cao, Schultz and Beck (1991), Lalli (1997) and Zhang, Ywo, Khoo and Chong (1999), which moves the computing nodes away from

[1] Department of Mechanical and Mechatronic Engineering, Taiwan Ocean University, Keelung, Taiwan. E-mail: csliu@mail.ntou.edu.tw

the boundary and outside the real domain of the problem. Even, this new approach can overcome the difficulties of singular integrals, it has another problem of the ill-posedness due to the appearance of the first-kind Fredholm integral equations. Conversely, Young (1999), Young, Chen and Lee (2005) and Young, Hwang, Tsai and Lu (2005) have applied the desingularized boundary integral equation method to the potential problems. In these approaches the source points are located in the real boundary, and they regularized the singular integrals by using the Gauss' flux theorem and other property derived from the potential theory.

Our starting point is similar to the Trefftz method. However, when our method basing on the separation of variables technique requires to meet both the specific geometry and boundary conditions, the Trefftz method just satisfies the governing equation and the unknown coefficients are determined by satisfying the boundary conditions in some manners as by means of the collocation, the least square or the Galerkin method; see, e.g., Kita and Kamiya (1995). Huang and Shaw (1995) have derived an integral representation of the Trefftz method on the so-called embedding surface. However, as remarked by Huang and Shaw (1995) their method is simply an alternative derivation of the Trefftz method.

On the other hand, the method of fundamental solutions (MFS) approximates the solution by a linear combination of fundamental solutions with singularities, as the source points located on a fictious boundary outside the domain of the problem; see, e.g., Fairweather and Karageorghis (1998). Because the MFS is an inherently meshless boundary method and has exponential convergence property for smooth solutions, it has been used extensively for solving the Laplace equation; see, e.g., Saavedra and Power (2003). Although the MFS can avoid the difficulities associated with BEM, it still has the problem that the resulting linear equations system may become highly ill-conditioned when the number of source points is increased [Golberg and Chen (1996)].

Basically, those methods discretized the governing equations into a linear equations system in an

earlier stage, and not to be continued into a further stage by deriving integral equations as we will do in this paper. Therefore, in doing so many inherent drawbacks of those methods can be avoided here by the new method, from which we could provide a semi-analytical solution of the unknown functions on the artifical circles. The semi-analytical method is in essence an approximation method aiming to find a relatively simple formula for the solution and, at the same time to reatin the main feature of exact solution.

An improved method than the MFS is the so-called boundary knot method [Chen and Tanaka (2002); Jin and Chen (2006)] or the boundary collocation method [Chen, Chang, Chen and Lin (2002); Chen, Chang, Chen and Chen (2002)]. Instead of the singular fundamental solutions, those methods employed the non-singular kernels to evaluate the homogeneous solutions. However, as pointed out by Young, Chen and Lee (2005) the introduction of non-singular kernels as the radial basis functions may jeopardize the accuracy of solutions as compared with the MFS.

This paper will formulate the Laplace equation in the doubly-connected domain by a meshless regularized integral equations method (MRIEM). These integral equations are singular-free and the kernels are degenerate. Moreover, the new method is also applicable to the problem with non-smooth boundary curves, even many boundary-type methods are inefficient for such cases. Owing to these good properties the new method using the Fourier series and the Fourier coefficients can be easily used to derive the meshless numerical method of the semi-analytical type.

We divide this paper into two main parts. In Part one, we propose a novel integral equation without singularity to treat the Laplace equation in the doubly-connected domain with outer boundary being a circle whilst the inner boundary is allowing to be any simple closed curve. This part includes six sections which are arranged as follows. In Section 2 we derive the first kind Fredholm intergral equation along a given artificial circle. In Section 3 we consider a Nyström approximate solution of the second kind Fredholm intergral equation. Then, we derive a two-point bound-

ary value problem in Section 4, which helps us to derive a semi-analytical solution of the second kind Fredholm intergral equation in Section 5. In Section 6 we apply the conjugate gradient method to a normal equation to obtain the Fourier coefficients of the unknown function. In Section 7 we use some examples to test the new method.

In Part two, we extend the results in Part one to treat the Laplace equation in the doubly-connected domain with both inner and outer boundaries being allowed to be any simple closed curves. This part includes four sections, which is arranged as follows. In Section 8 we derive two coupled Fredholm integral equations of the first kind. Then we derive a two-point boundary value problem in Section 9. In Section 10 we apply the conjugate gradient method to the normal equation to obtain the Fourier coefficients of the unknown functions in two artificial circles. In Section 11 we use some examples to test the new method. Finally, some conclusions are given in Section 12.

Part one: one integral equation

2 The Fredholm integral equation

The first problem we consider is the Laplace equation equipped with the Dirichlet boundary conditions at an external circle and at a simple closed interior boundary:

$$\Delta u = u_{rr} + \frac{1}{r}u_r + \frac{1}{r^2}u_{\theta\theta} = 0, \tag{1}$$

$$u(r_1, \theta) = g(\theta), \ 0 \le \theta \le 2\pi, \tag{2}$$

$$u(r_3, \theta) = h_1(\theta), \ 0 \le \theta \le 2\pi, \tag{3}$$

where $g(\theta)$ and $h_1(\theta)$ are given functions. Here, $(r_1, \theta), \ 0 \le \theta \le 2\pi$ with a constant r_1 is an external circle, and $r_3 = r_3(\theta) < r_1$ is a simple curve inside the external circle as shown in Fig. 1(a). In the recent papers by the author [Liu (2007a, 2007b)], the Laplace equation is solved by the Fredholm integral equation method for the elastic torsion problem and in the doubly connected domain by using the modified indirect Trefftz method.

We temporarily replace Eq. (3) by the following boundary condition:

$$u(r_2, \theta) = f(\theta), \ 0 \le \theta \le 2\pi, \tag{4}$$
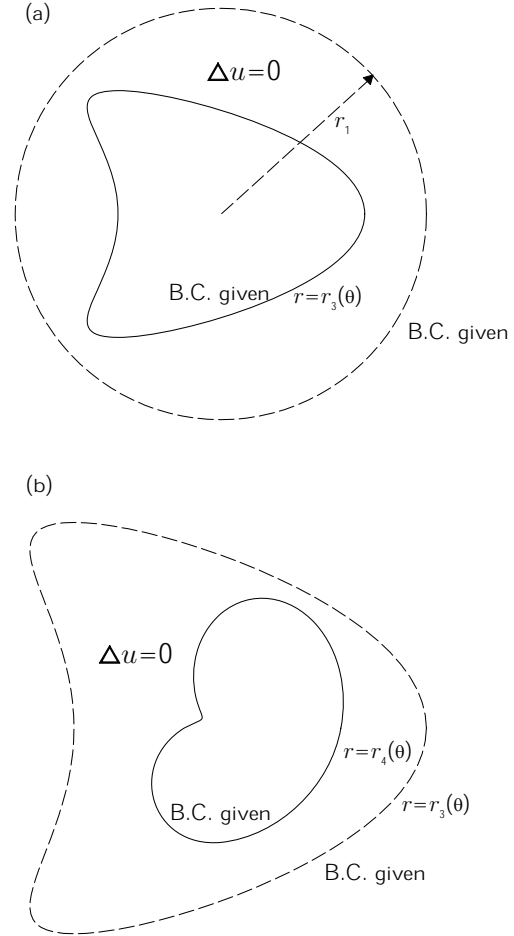
Figure 1: Schematic drawing to show the doubly-connected regions, where we solve the Laplace equation by the new methods for (a) with one integral equation, and (b) with two coupled integral equations.

where $f(\theta)$ is an unknown function to be determined, and the inner circle $(r_2, \theta), \ 0 \le \theta \le 2\pi$ with a constant $r_2 < r_3$ is inside the domain enclosed by $r_3(\theta)$.

Therefore, by utilizing the technique of separation of variables we can write a series expansion of $u(r, \theta)$ satisfying Eqs. (1), (2) and (4):

$$u(r, \theta) = \frac{1}{2}(a_0 + b_0 \ln r) +$$

$$\sum_{k=1}^{\infty} [(a_k r^k + b_k r^{-k})\cos k\theta + (c_k r^k + d_k r^{-k})\sin k\theta], \tag{5}$$

where

$$a_0 = \frac{1}{\pi(\ln r_1 - \ln r_2)}$$
$$\cdot \left[\ln r_1 \int_0^{2\pi} f(\xi)d\xi - \ln r_2 \int_0^{2\pi} g(\xi)d\xi \right], \quad (6)$$

$$b_0 = \frac{1}{\pi(\ln r_1 - \ln r_2)}$$
$$\cdot \left[\int_0^{2\pi} g(\xi)d\xi - \int_0^{2\pi} f(\xi)d\xi \right], \quad (7)$$

$$a_k = \frac{e_k}{r_2^k} \int_0^{2\pi} g(\xi)\cos k\xi d\xi$$
$$- \frac{e_k}{r_1^k} \int_0^{2\pi} f(\xi)\cos k\xi d\xi, \quad (8)$$

$$b_k = e_k r_1^k \int_0^{2\pi} f(\xi)\cos k\xi d\xi$$
$$- e_k r_2^k \int_0^{2\pi} g(\xi)\cos k\xi d\xi, \quad (9)$$

$$c_k = \frac{e_k}{r_2^k} \int_0^{2\pi} g(\xi)\sin k\xi d\xi$$
$$- \frac{e_k}{r_1^k} \int_0^{2\pi} f(\xi)\sin k\xi d\xi, \quad (10)$$

$$d_k = e_k r_1^k \int_0^{2\pi} f(\xi)\sin k\xi d\xi$$
$$- e_k r_2^k \int_0^{2\pi} g(\xi)\sin k\xi d\xi, \quad (11)$$

in which

$$e_k := \frac{1}{\pi \left[\left(\frac{r_1}{r_2}\right)^k - \left(\frac{r_2}{r_1}\right)^k \right]}. \quad (12)$$

By imposing the condition (3) on Eq. (5) we obtain

$$\frac{1}{2}(a_0 + b_0 \ln r_3) + \sum_{k=1}^{\infty} [(a_k r_3^k + b_k r_3^{-k})\cos k\theta$$
$$+ (c_k r_3^k + d_k r_3^{-k})\sin k\theta] = h_1(\theta). \quad (13)$$

Substituting Eqs. (6)-(11) into Eq. (13) leads to a first kind Fredholm integral equation:

$$\int_0^{2\pi} K(\theta, \xi)f(\xi)d\xi = h(\theta), \quad (14)$$

where

$$h(\theta) := h_1(\theta) + \frac{\ln r_2 - \ln r_3}{2\pi(\ln r_1 - \ln r_2)} \int_0^{2\pi} g(\xi)d\xi$$
$$+ \sum_{k=1}^{\infty} \left\{ A_k \left(\int_0^{2\pi} g(\xi)\cos k\xi d\xi \cos k\theta \right. \right.$$
$$\left. \left. + \int_0^{2\pi} g(\xi)\sin k\xi d\xi \sin k\theta \right) \right\} \quad (15)$$

is the source function fully available after inserting the give function $g(\theta)$, and

$$K(\theta, \xi) = \frac{\ln r_1 - \ln r_3}{2\pi(\ln r_1 - \ln r_2)}$$
$$+ \sum_{k=1}^{\infty} \left\{ B_k [\cos k\theta \cos k\xi + \sin k\theta \sin k\xi] \right\} \quad (16)$$

is a kernel function. Here,

$$A_k := e_k(r_3^{-k}r_2^k - r_3^k r_2^{-k}), \quad (17)$$
$$B_k := e_k(r_3^{-k}r_1^k - r_3^k r_1^{-k}) \quad (18)$$

are both functions of θ due to the dependence of r_3 on θ.

In order to obtain $f(\theta)$ we have to solve the first kind Fredholm integral equation (14). We assume that there exists a regularized parameter α, such that Eq. (14) can be regularized by

$$\alpha f(\theta) + \int_0^{2\pi} K(\theta, \xi)f(\xi)d\xi = h(\theta), \quad (19)$$

which is known as one of the second type Fredholm integral equation. The above regularization method to obtain a regularized solution by solving the perturbed equation is usually called the Lavrentiev regularization method [Lavrentiev (1967)].

3 The Nyström method

In this section we first provide a numerical method to solve Eq. (19). The range $[0, 2\pi]$ is divided into $n-1$ subintervals with $\Delta\theta = 2\pi/(n-$

1) and $\theta_i = (i-1)\Delta\theta$. The numerical value of $f(\theta)$ at the i-th grid point is denoted by $f_i = f(\theta_i)$, and there are totally n unknowns $f_1, f_2, \ldots, f_n$. Then, we apply the Nyström method with trapezoidal quadrature on the integral term in Eq. (19), which results in

$$\alpha f_i + \Delta\theta \left[\frac{1}{2}K_{i1}f_1 + \sum_{j=2}^{n-1} K_{ij}f_j + \frac{1}{2}K_{in}f_n \right] = h_i,$$
$$i = 1, \ldots, n, \quad (20)$$

where $K_{ij} := K(\theta_i, \theta_j)$ and $h_i := h(\theta_i)$.

The above system can be rearranged into a linear equations system:

$$\mathbf{Ax} = \mathbf{b}, \quad (21)$$

where

$$\mathbf{A} := \Delta\theta \begin{bmatrix} \alpha_0 + \frac{1}{2}K_{11} & K_{12} & \cdots & \frac{1}{2}K_{1n} \\ \frac{1}{2}K_{21} & \alpha_0 + K_{22} & \cdots & \frac{1}{2}K_{2n} \\ \vdots & \vdots & \vdots & \vdots \\ \frac{1}{2}K_{n1} & K_{n2} & \cdots & \alpha_0 + \frac{1}{2}K_{nn} \end{bmatrix}$$

$$\mathbf{b} := \begin{bmatrix} h_1 \\ h_2 \\ \vdots \\ h_n \end{bmatrix},$$
$$(22)$$

in which $\alpha_0 = \alpha/\Delta\theta$ and $\mathbf{x} = (f_1, f_2, \ldots, f_n)^\mathrm{T}$. For the details of solvability and the error analysis for Nyström's method, the readers may refer to [Kress (1989)].

There are several methods to deal with Eq. (21). Here, we consider an iterative method for Eq. (21) by integrating the following equation:

$$\dot{\mathbf{x}} = \mathbf{b} - \mathbf{Ax} =: \mathbf{f}(\mathbf{x}), \quad (23)$$

until $\|\dot{\mathbf{x}}\|$ is smaller enough than a given criterion with $\|\dot{\mathbf{x}}\| < \varepsilon$. The fixed point, i.e. $\mathbf{f}(\mathbf{x}) = 0$, of the above equation is the solution of Eq. (21). When t approach infinity we expect that $\mathbf{x}$ tends to the solution of Eq. (21).

A nonstandard group preserving scheme (NGPS) for Eq. (23) has been developed by Liu (2001, 2005),

$$\mathbf{x}_{k+1} = \mathbf{x}_k + \frac{4\|\mathbf{x}_k\|^2 + 2\phi\mathbf{f}_k \cdot \mathbf{x}_k}{4\|\mathbf{x}_k\|^2 - \phi^2\|\mathbf{f}_k\|^2}\phi\mathbf{f}_k, \quad (24)$$

where

$$\phi(\Delta t) := \frac{1 - \exp(-\rho\Delta t)}{\rho}, \quad (25)$$

and ρ can be a number not smaller than the Lipschitz constant of Eq. (23):

$$\mathscr{L} = \|\mathbf{A}\| \geq \max\{|\lambda_i| : i = 1, 2, \ldots, n\}. \quad (26)$$

The iteration method in Eq. (24) is unconditional stable.

4 Two-point boundary value problem

We assume that the kernel function can be approximated by m terms with

$$K(\theta, \xi) = \frac{\ln r_1 - \ln r_3}{2\pi(\ln r_1 - \ln r_2)}$$
$$+ \sum_{k=1}^{m} \left\{ B_k \left[\cos k\theta \cos k\xi + \sin k\theta \sin k\xi \right] \right\}. \quad (27)$$

This assumption is for the convenience of our derivation but is not essential. After we have obtained an analytical solution we can let $m = \infty$ again. The kernel function as can be seen is termwise separable, which is also called the degenerate kernel [Kress (1989)].

By inspection we have

$$K(\theta, \xi) = \mathbf{P}(\theta) \cdot \mathbf{Q}(\xi), \quad (28)$$

where $\mathbf{P}$ and $\mathbf{Q}$ are $2m+1$-vectors given by

$$\mathbf{P} := \begin{bmatrix} \frac{\ln r_1 - \ln r_3}{2\pi(\ln r_1 - \ln r_2)} \\ B_1\cos\theta \\ B_1\sin\theta \\ B_2\cos 2\theta \\ B_2\sin 2\theta \\ \vdots \\ B_m\cos m\theta \\ B_m\sin m\theta \end{bmatrix}, \quad \mathbf{Q} := \begin{bmatrix} 1 \\ \cos\xi \\ \sin\xi \\ \cos 2\xi \\ \sin 2\xi \\ \vdots \\ \cos m\xi \\ \sin m\xi \end{bmatrix}, \quad (29)$$

and the dot between $\mathbf{P}$ and $\mathbf{Q}$ denotes the inner product, which is sometimes written as $\mathbf{P}^\mathrm{T}\mathbf{Q}$ for convenience, where the superscript T signifies the transpose.

With the aid of Eq. (28), Eq. (19) can be decomposed as

$$\alpha f(\theta) + \int_0^\theta \mathbf{P}^T(\theta)\mathbf{Q}(\xi)f(\xi)d\xi$$
$$+ \int_\theta^{2\pi} \mathbf{P}^T(\theta)\mathbf{Q}(\xi)f(\xi)d\xi = h(\theta). \quad (30)$$

Upon letting

$$\mathbf{u}_1(\theta) := \int_0^\theta \mathbf{Q}(\xi)f(\xi)d\xi, \quad (31)$$

$$\mathbf{u}_2(\theta) := \int_{2\pi}^\theta \mathbf{Q}(\xi)f(\xi)d\xi, \quad (32)$$

Eq. (30) can be expressed as

$$\alpha f(\theta) + \mathbf{P}^T(\theta)[\mathbf{u}_1(\theta) - \mathbf{u}_2(\theta)] = h(\theta). \quad (33)$$

Taking the differentials of Eqs. (31) and (32) with respect to θ we obtain

$$\mathbf{u}_1'(\theta) = \mathbf{Q}(\theta)f(\theta), \quad (34)$$
$$\mathbf{u}_2'(\theta) = \mathbf{Q}(\theta)f(\theta). \quad (35)$$

Inserting Eq. (33) for $f(\theta)$ into the above two equations we obtain

$$\alpha\mathbf{u}_1'(\theta) = \mathbf{Q}(\theta)\mathbf{P}^T(\theta)[\mathbf{u}_2(\theta) - \mathbf{u}_1(\theta)]$$
$$+ h(\theta)\mathbf{Q}(\theta), \quad \mathbf{u}_1(0) = \mathbf{0}, \quad (36)$$

$$\alpha\mathbf{u}_2'(\theta) = \mathbf{Q}(\theta)\mathbf{P}^T(\theta)[\mathbf{u}_2(\theta) - \mathbf{u}_1(\theta)]$$
$$+ h(\theta)\mathbf{Q}(\theta), \quad \mathbf{u}_2(2\pi) = \mathbf{0}, \quad (37)$$

where the last two conditions follow from Eqs. (31) and (32) readily. The above two equations constitute a two-point boundary value problem.

5 A semi-analytical solution

In this section we will find a solution of $f(\theta)$. From Eqs. (34) and (35) it can be seen that $\mathbf{u}_1' = \mathbf{u}_2'$, which means that

$$\mathbf{u}_1 = \mathbf{u}_2 + \mathbf{c}, \quad (38)$$

where $\mathbf{c}$ is a constant vector to be determined. By using the final condition in Eq. (37) we find that

$$\mathbf{u}_1(2\pi) = \mathbf{u}_2(2\pi) + \mathbf{c} = \mathbf{c}. \quad (39)$$

Substituting Eq. (38) into (36) we have

$$\alpha\mathbf{u}_1'(\theta) = -\mathbf{Q}(\theta)\mathbf{P}^T(\theta)\mathbf{c} + h(\theta)\mathbf{Q}(\theta),$$
$$\mathbf{u}_1(0) = \mathbf{0}. \quad (40)$$

Integrating and using the initial condition it follows that

$$\mathbf{u}_1(\theta) = \frac{-1}{\alpha} \int_0^\theta \mathbf{Q}(\xi)\mathbf{P}^T(\xi)d\xi\mathbf{c}$$
$$+ \frac{1}{\alpha} \int_0^\theta h(\xi)\mathbf{Q}(\xi)d\xi. \quad (41)$$

Taking $\theta = 2\pi$ in the above equation and imposing the condition (39) we can obtain a governing equation for $\mathbf{c}$:

$$\left(\alpha\mathbf{I}_{2m+1} + \int_0^{2\pi} \mathbf{Q}(\xi)\mathbf{P}^T(\xi)d\xi\right)\mathbf{c}$$
$$= \int_0^{2\pi} h(\xi)\mathbf{Q}(\xi)d\xi. \quad (42)$$

It is straightforward to write

$$\mathbf{c} = \left(\alpha\mathbf{I}_{2m+1} + \int_0^{2\pi} \mathbf{Q}(\xi)\mathbf{P}^T(\xi)d\xi\right)^{-1}$$
$$\cdot \int_0^{2\pi} h(\xi)\mathbf{Q}(\xi)d\xi. \quad (43)$$

On the other hand, from Eqs. (33) and (38) we have

$$\alpha f(\theta) = h(\theta) - \mathbf{P}(\theta) \cdot \mathbf{c}. \quad (44)$$

Inserting Eq. (43) for $\mathbf{c}$ into the above equation we can obtain a solution of $f(\theta)$.

From Eqs. (31) and (39) it follows that

$$\mathbf{c} = \int_0^{2\pi} \mathbf{Q}(\xi)f(\xi)d\xi. \quad (45)$$

Upon reminding Eq. (29), it can be understood that $\mathbf{c}$ is the vector composed of the Fourier coefficients of the unknown function $f(\theta)$. Meanwhile, Eq. (43) describes the relation between the Fourier coefficients of the boundary data on an artifical circle and the boundary data on the real boundaries.

6   The conjugate gradient method

In the above we have derived Eq. (43) to calculate **c**, and Eq. (44) to calculate $f(\theta)$. An efficient numerical procedure can be derived as follows.

Instead of Eq. (43) we consider the normal equation:

$$\mathbf{Ac} = \mathbf{b}, \tag{46}$$

where

$$\mathbf{R} := \alpha \mathbf{I}_{2m+1} + \int_0^{2\pi} \mathbf{Q}(\xi)\mathbf{P}^\mathrm{T}(\xi)d\xi, \tag{47}$$

$$\mathbf{A} := \mathbf{R}^\mathrm{T}\mathbf{R}, \tag{48}$$

$$\mathbf{b} := \mathbf{R}^\mathrm{T} \int_0^{2\pi} h(\xi)\mathbf{Q}(\xi)d\xi. \tag{49}$$

The conjugate gradient method is summarized as follows:

(i) Give an initial $\mathbf{c}_0$.

(ii) Calculate $\mathbf{r}_0 = \mathbf{b} - \mathbf{Ac}_0$ and $\mathbf{p}_1 = \mathbf{r}_0$.

(iii) For $k = 1, 2 \ldots$ we repeat the following calculations:

$$\eta_k = \frac{\|\mathbf{r}_{k-1}\|^2}{\mathbf{p}_k^\mathrm{T}\mathbf{Ap}_k}, \tag{50}$$

$$\mathbf{c}_k = \mathbf{c}_{k-1} + \eta_k \mathbf{p}_k, \tag{51}$$

$$\mathbf{r}_k = \mathbf{r}_{k-1} - \eta_k \mathbf{Ap}_k, \tag{52}$$

$$a_k = \frac{\|\mathbf{r}_k\|^2}{\|\mathbf{r}_{k-1}\|^2}, \tag{53}$$

$$\mathbf{p}_{k+1} = \mathbf{p}_k + a_k \mathbf{p}_k. \tag{54}$$

If $\mathbf{c}_k$ converges according to a given stopping criterion:

$$\|\mathbf{c}_{k+1} - \mathbf{c}_k\| < \varepsilon, \tag{55}$$

then stop; otherwise, go to step (iii).

7   Numerical test I

7.1   *Example 1*

In order to illustrate the performance of the new method and compare our numerical result with exact solution, we first consider a simple problem with the following data:

$$u(r_1, \theta) = g(\theta) = \cos 2\theta, \ \ 0 \le \theta \le 2\pi, \tag{56}$$

$$u(r_2, \theta) = f(\theta) = -\cos 2\theta, \ \ 0 \le \theta \le 2\pi. \tag{57}$$

Then from Eqs. (6)-(11) we obtain

$$a_2 = \frac{\pi e_2}{r_1^2} + \frac{\pi e_2}{r_2^2}, \tag{58}$$

$$b_2 = -\pi e_2 r_1^2 - \pi e_2 r_2^2, \tag{59}$$

and the other coefficients are all zero. Therefore, we have a closed-form solution:

$$u(r, \theta) = \pi e_2 \left[\frac{1}{r_1^2} + \frac{1}{r_2^2} \right] r^2 \cos 2\theta$$
$$- \pi e_2 (r_1^2 + r_2^2) r^{-2} \cos 2\theta. \tag{60}$$

When $r = r_3 = \sqrt{r_1 r_2}$, we have

$$u(r_3, \theta) = h_1(\theta) = 0, \tag{61}$$

and from Eq. (15) it follows that

$$h(\theta) = \pi A_2 \cos 2\theta = \pi e_2 \left[\frac{r_2^2}{r_3^2} - \frac{r_3^2}{r_2^2} \right] \cos 2\theta. \tag{62}$$

Now, we can estimate the boundary condition $f(\theta)$ on the circle $r = r_2$ by the numerical method in Section 3. For definite we let $r_1 = 1$ and $r_2 = 0.49$ and hence $r_3 = 0.7$. By applying the numerical method we let $m = 100$, $\alpha = 0.01$, $\Delta t = 0.1$ and $\rho = 500$. Through about 150 iterations the solution of f by Eq. (24) is convergent according to a stopping criterion with $\varepsilon = 0.01$. The numerical result of f and the exact one calculated from Eq. (60) by inserting $r = 0.49$ are compared in Fig. 2(a). Then, we can calculate the semi-analytical numerical solution of u by Eq. (5), where the summation is taken up to $m = 100$ terms, and all the coefficients are obtained from the numerical integrations by applying a simple trapezoidal quadrature over 100 subintervals in the range $[0, 2\pi]$. The numerical result of u along a circle with a radius $r = r_1 = 1$ and the exact one calculated from Eq. (60) by inserting $r = 1$ are compared in Fig. 2(b). It can be seen that these two curves coincide very well. In order to assess the numerical accuracy, we also plotted the

numerical error in Fig. 2(c), which is defined by the absolute difference between numerical solution and exact solution. It gives very excellent numerical solution with the error very small in the order of 10^{-16}.
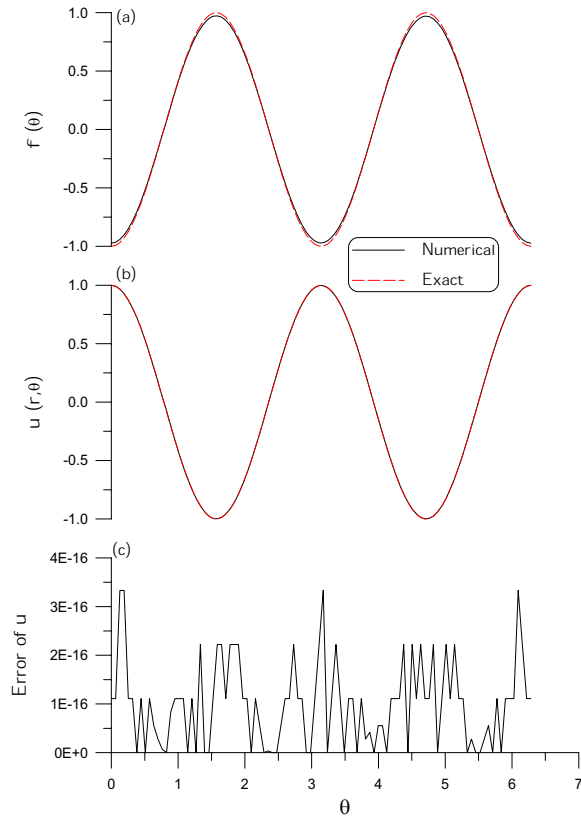
Figure 2: For Example 1 comparing (a) the function $f(\theta)$ of numerical and exact, (b) the numerical and exact solutions, and (c) plotting the numerical error of solution.

7.2 Example 2

We consider a kite-shape cavity with the parameterization given by

$$r_3 =$$
$$\sqrt{(0.6\cos\theta + 0.3\cos 2\theta - 0.2)^2 + (0.6\sin\theta)^2}, \tag{63}$$

$$x_3(\theta) = r_3\cos\theta, \quad y_3(\theta) = r_3\sin\theta, \tag{64}$$
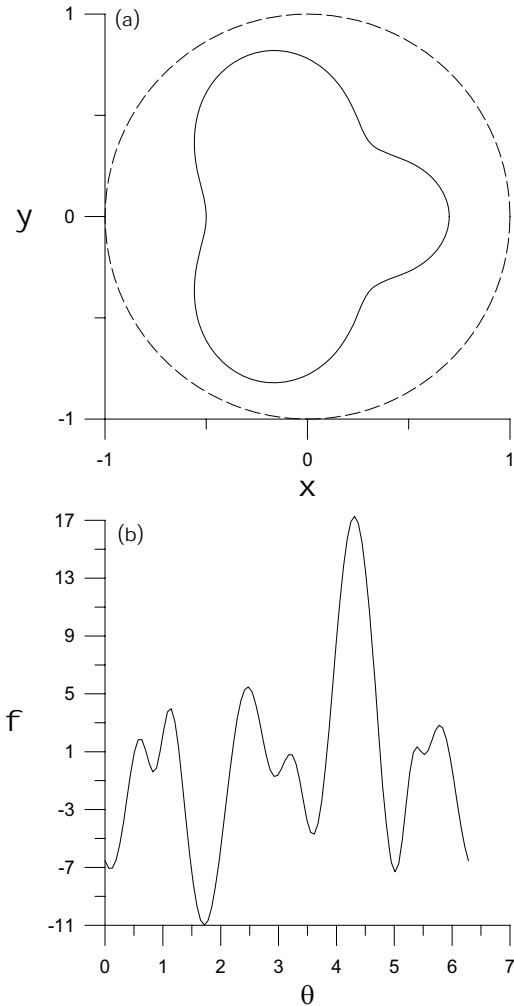
Figure 3: For Example 2 we plotting (a) the doubly-connected region of the problem, and (b) the function $f(\theta)$ calculated by NGPS.

and with the boundary conditions:

$$u(r_1, \theta) = g(\theta) = \cos\theta + \sin\theta, \tag{65}$$
$$u(r_3, \theta) = h_1(\theta) = 0. \tag{66}$$

The doubly-connected region with the outer circle a radius $r_1 = 1$ and with the kite-shape inner boundary was shown in Fig. 3(a).

Therefore, from Eq. (15) we have

$$h(\theta) = \pi A_1(\cos\theta + \sin\theta)$$
$$= \pi e_1(\cos\theta + \sin\theta)\left[\frac{r_2}{r_3} - \frac{r_3}{r_2}\right]. \tag{67}$$

Substituting Eq. (65) for g into Eqs. (6)-(11) we

have

$$a_0 = \frac{\ln r_1}{\pi(\ln r_1 - \ln r_2)} \int_0^{2\pi} f(\xi)d\xi, \qquad (68)$$

$$b_0 = -\frac{1}{\pi(\ln r_1 - \ln r_2)} \int_0^{2\pi} f(\xi)d\xi, \qquad (69)$$

$$a_k = \frac{\pi e_k}{r_2^k}\delta_{k,1} - \frac{e_k}{r_1^k}\int_0^{2\pi} f(\xi)\cos k\xi d\xi, \qquad (70)$$

$$b_k = e_k r_1^k \int_0^{2\pi} f(\xi)\cos k\xi d\xi - \pi e_k r_2^k \delta_{k,1}, \qquad (71)$$

$$c_k = \frac{\pi e_k}{r_2^k}\delta_{k,1} - \frac{e_k}{r_1^k}\int_0^{2\pi} f(\xi)\sin k\xi d\xi, \qquad (72)$$

$$d_k = e_k r_1^k \int_0^{2\pi} f(\xi)\sin k\xi d\xi - \pi e_k r_2^k \delta_{k,1}. \qquad (73)$$

We first solve $f(\theta)$ from Eq. (14) by the NGPS in Section 3, whose result is shown in Fig. 3(b) under the parameters $r_2 = 0.3$, $m = 100$, $\alpha = 0.01$, $\Delta t = 0.1$ and $\rho = 2$. Through about 500 iterations the solution of f by Eq. (24) is convergent according to a stopping criterion with $\varepsilon = 0.5$. Because there has no closed-form solution for this case, we compare the exact **b** and the numerical **b = Ax** in Fig. 4(a). It can be seen that these two curves are close. Then substituting $f(\theta)$ into the above equations and through numerical integrations we can obtain the coefficients required in the numerical solution of u, of which a numerical solution along a circle with a radius $r = 0.9$ was plotted in Fig. 4(b).

7.3 Example 3

Let us consider an ellipse with semiaxes a and b the inner boundary, which in the polar coordinates is described by

$$r_3(\theta) = \frac{ab}{\sqrt{a^2\sin^2\theta + b^2\cos^2\theta}}. \qquad (74)$$

For this example we consider the boundary conditions:

$$g(\theta) = u(r_1, \theta) = \frac{a^2 b^2}{a^2 + b^2} + \frac{a^2 - b^2}{2(a^2 + b^2)}r_1^2\cos 2\theta, \qquad (75)$$

$$h_1(\theta) = u(r_3, \theta) = \frac{a^2 b^2}{2(a^2\sin^2\theta + b^2\cos^2\theta)}, \qquad (76)$$
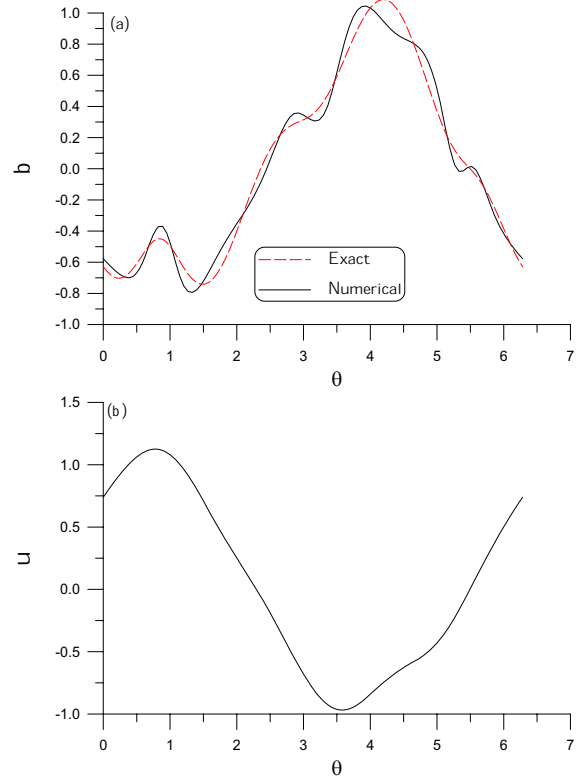
Figure 4: For Example 2: (a) comparing the numerical and exact **b**, and (b) plotting the numerical solution.

where $r_1 > a$ is the radius of the outer circle. The exact solution of u is

$$u(r,\theta) = \frac{a^2 b^2}{a^2 + b^2} + \frac{a^2 - b^2}{2(a^2 + b^2)}r^2\cos 2\theta. \qquad (77)$$

From Eq. (15) we have

$$h(\theta) =$$

$$\frac{a^2 b^2}{2(a^2\sin^2\theta + b^2\cos^2\theta)} + \frac{a^2 b^2(\ln r_2 - \ln r_3)}{(\ln r_1 - \ln r_2)(a^2 + b^2)}$$

$$+ \frac{\pi(a^2 - b^2)A_2 r_1^2}{2(a^2 + b^2)}\cos 2\theta. \qquad (78)$$

Substituting Eq. (75) for g into Eqs. (6)-(11) leads to

$$a_0 = \frac{\ln r_1}{\pi(\ln r_1 - \ln r_2)}\int_0^{2\pi} f(\xi)d\xi$$

$$- \frac{2\ln r_2 a^2 b^2}{(\ln r_1 - \ln r_2)(a^2 + b^2)}, \qquad (79)$$

$$b_0 = \frac{2a^2b^2}{(\ln r_1 - \ln r_2)(a^2 + b^2)}$$
$$- \frac{1}{\pi(\ln r_1 - \ln r_2)} \int_0^{2\pi} f(\xi)d\xi, \quad (80)$$

$$a_k = \frac{\pi e_k r_1^2 (a^2 - b^2)}{2r_2^k(a^2 + b^2)} \delta_{k,2} - \frac{e_k}{r_1^k} \int_0^{2\pi} f(\xi)\cos k\xi d\xi,$$
$$(81)$$

$$b_k = e_k r_1^k \int_0^{2\pi} f(\xi)\cos k\xi d\xi$$
$$- \frac{\pi e_k r_2^k r_1^2 (a^2 - b^2)}{2(a^2 + b^2)} \delta_{k,2}, \quad (82)$$

$$c_k = -\frac{e_k}{r_1^k} \int_0^{2\pi} f(\xi)\sin k\xi d\xi, \quad (83)$$

$$d_k = e_k r_1^k \int_0^{2\pi} f(\xi)\sin k\xi d\xi. \quad (84)$$

We have applied the numerical method in Section 6 on this example. The parameters used in this calculation are $m = 10$, $a = 2$, $b = 1$, $r_1 = 3$, $r_2 = 0.5$ and $\alpha = 0.008$, and only two iterations are required to calculate $\mathbf{c}$, which starting from an initial $\mathbf{c} = \mathbf{0}$. In Fig. 5(a) the function $f(\theta)$ is plotted. In Fig. 5(b) the numerical result of $u(r, \theta)$ along a circle with a radius $r = 2.5$ is compared with the exact one, which is obtained from Eq. (77) by inserting $r = 2.5$. The numerical error as shown in Fig. 5(c) is in the order of 10^{-3} and the numerical solution is rather accurate. The main error is due to the numerical integrations of Eqs. (79)-(84), of which we use 150 subintervals in the trapezoidal quadratures.

Part two: two integral equations

8   The problem in doubly-connected domain

The problem of the Laplace equation in a doubly-connected domain as shown in Fig. 1(b) for an example is formulated by imposing the Dirichlet data at an exterior boundary and at an interior boundary:

$$u(r_3, \theta) = h_3(\theta), \ 0 \le \theta \le 2\pi, \quad (85)$$
$$u(r_4, \theta) = h_4(\theta), \ 0 \le \theta \le 2\pi, \quad (86)$$
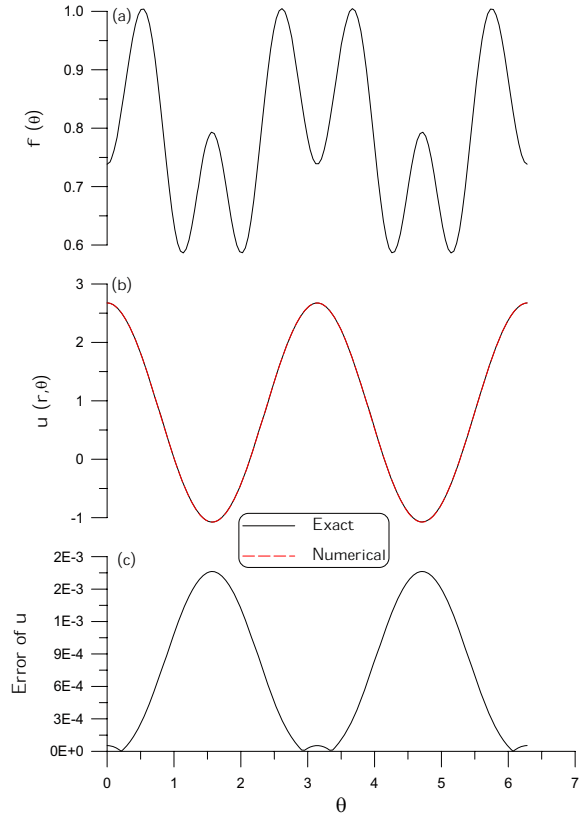
Figure 5: For Example 3: (a) plotting the function $f(\theta)$, (b) comparing the numerical and exact solutions, and (c) plotting the numerical error of solution.

where $h_3(\theta)$ and $h_4(\theta)$ are given functions, and both $r_3 = r_3(\theta)$ and $r_4 = r_4(\theta)$ are simple curves with $r_4 = r_4(\theta)$ inside $r_3 = r_3(\theta)$, i.e., $r_4(\theta) < r_3(\theta)$, $0 \le \theta < 2\pi$.

We replace Eqs. (85) and (86) by the following boundary conditions:

$$u(r_1, \theta) = g(\theta), \ 0 \le \theta \le 2\pi, \quad (87)$$
$$u(r_2, \theta) = f(\theta), \ 0 \le \theta \le 2\pi, \quad (88)$$

where both $g(\theta)$ and $f(\theta)$ are unknown functions to be determined, and $r_2 < r_1$ are constants. The requirement is that the annular with radii r_2 and r_1 can cover the entire doubly-connected region.

By imposing conditions (85) and (86) on Eq. (5) and utilizing Eqs. (6)-(11) we can obtain two cou-

pled first kind Fredholm integral equations:

$$\int_0^{2\pi} K_1^3(\theta,\xi) f(\xi) d\xi - \int_0^{2\pi} K_2^3(\theta,\xi) g(\xi) d\xi$$
$$= h_3(\theta), \quad (89)$$

$$\int_0^{2\pi} K_1^4(\theta,\xi) f(\xi) d\xi - \int_0^{2\pi} K_2^4(\theta,\xi) g(\xi) d\xi$$
$$= h_4(\theta), \quad (90)$$

where

$$K_1^3(\theta,\xi) = \frac{\ln r_1 - \ln r_3}{2\pi(\ln r_1 - \ln r_2)}$$
$$+ \sum_{k=1}^{\infty} \left\{ B_k^3 \left[\cos k\theta \cos k\xi + \sin k\theta \sin k\xi \right] \right\}, \quad (91)$$

$$K_2^3(\theta,\xi) = \frac{\ln r_2 - \ln r_3}{2\pi(\ln r_1 - \ln r_2)}$$
$$+ \sum_{k=1}^{\infty} \left\{ A_k^3 \left[\cos k\theta \cos k\xi + \sin k\theta \sin k\xi \right] \right\}, \quad (92)$$

$$K_1^4(\theta,\xi) = \frac{\ln r_1 - \ln r_4}{2\pi(\ln r_1 - \ln r_2)}$$
$$+ \sum_{k=1}^{\infty} \left\{ B_k^4 \left[\cos k\theta \cos k\xi + \sin k\theta \sin k\xi \right] \right\}, \quad (93)$$

$$K_2^4(\theta,\xi) = \frac{\ln r_2 - \ln r_4}{2\pi(\ln r_1 - \ln r_2)}$$
$$+ \sum_{k=1}^{\infty} \left\{ A_k^4 \left[\cos k\theta \cos k\xi + \sin k\theta \sin k\xi \right] \right\} \quad (94)$$

are kernel functions, and

$$A_k^3 := e_k(r_3^{-k} r_2^k - r_3^k r_2^{-k}), \quad (95)$$
$$B_k^3 := e_k(r_3^{-k} r_1^k - r_3^k r_1^{-k}), \quad (96)$$
$$A_k^4 := e_k(r_4^{-k} r_2^k - r_4^k r_2^{-k}), \quad (97)$$
$$B_k^4 := e_k(r_4^{-k} r_1^k - r_4^k r_1^{-k}) \quad (98)$$

are all functions of θ due to $r_3(\theta)$ and $r_4(\theta)$.

9 Two-point boundary value problem

We assume that the kernel functions K_1^3, K_2^3, K_1^4 and K_2^4 can be approximated by m terms. By inspection we have

$$K_1^3(\theta,\xi) = \mathbf{P}_1(\theta) \cdot \mathbf{Q}(\xi), \quad (99)$$
$$K_2^3(\theta,\xi) = \mathbf{P}_2(\theta) \cdot \mathbf{Q}(\xi), \quad (100)$$
$$K_1^4(\theta,\xi) = \mathbf{P}_3(\theta) \cdot \mathbf{Q}(\xi), \quad (101)$$
$$K_2^4(\theta,\xi) = \mathbf{P}_4(\theta) \cdot \mathbf{Q}(\xi), \quad (102)$$

where $\mathbf{Q}$ is still defined in Eq. (29) and the others are given by

$$\mathbf{P}_1 := \begin{bmatrix} \frac{\ln r_1 - \ln r_3}{2\pi(\ln r_1 - \ln r_2)} \\ B_1^3 \cos\theta \\ B_1^3 \sin\theta \\ B_2^3 \cos 2\theta \\ B_2^3 \sin 2\theta \\ \vdots \\ B_m^3 \cos m\theta \\ B_m^3 \sin m\theta \end{bmatrix}, \quad \mathbf{P}_2 := \begin{bmatrix} \frac{\ln r_2 - \ln r_3}{2\pi(\ln r_1 - \ln r_2)} \\ A_1^3 \cos\theta \\ A_1^3 \sin\theta \\ A_2^3 \cos 2\theta \\ A_2^3 \sin 2\theta \\ \vdots \\ A_m^3 \cos m\theta \\ A_m^3 \sin m\theta \end{bmatrix}, \quad (103)$$

$$\mathbf{P}_3 := \begin{bmatrix} \frac{\ln r_1 - \ln r_4}{2\pi(\ln r_1 - \ln r_2)} \\ B_1^4 \cos\theta \\ B_1^4 \sin\theta \\ B_2^4 \cos 2\theta \\ B_2^4 \sin 2\theta \\ \vdots \\ B_m^4 \cos m\theta \\ B_m^4 \sin m\theta \end{bmatrix}, \quad \mathbf{P}_4 := \begin{bmatrix} \frac{\ln r_2 - \ln r_4}{2\pi(\ln r_1 - \ln r_2)} \\ A_1^4 \cos\theta \\ A_1^4 \sin\theta \\ A_2^4 \cos 2\theta \\ A_2^4 \sin 2\theta \\ \vdots \\ A_m^4 \cos m\theta \\ A_m^4 \sin m\theta \end{bmatrix}. \quad (104)$$

The regularizations of Eqs. (89) and (90) are given by

$$\alpha f(\theta) + \int_0^{2\pi} K_1^3(\theta,\xi) f(\xi) d\xi$$
$$- \int_0^{2\pi} K_2^3(\theta,\xi) g(\xi) d\xi = h_3(\theta), \quad (105)$$

$$\beta g(\theta) + \int_0^{2\pi} K_1^4(\theta,\xi) f(\xi) d\xi$$
$$- \int_0^{2\pi} K_2^4(\theta,\xi) g(\xi) d\xi = h_4(\theta), \quad (106)$$

where α and β can be different values.

With the aid of Eqs. (99)-(104), Eqs. (105) and (106) can be decomposed as

$$
\alpha f(\theta) + \int_0^\theta \mathbf{P}_1^{\mathrm{T}}(\theta)\mathbf{Q}(\xi)f(\xi)d\xi
$$
$$
+ \int_\theta^{2\pi} \mathbf{P}_1^{\mathrm{T}}(\theta)\mathbf{Q}(\xi)f(\xi)d\xi
$$
$$
- \int_0^\theta \mathbf{P}_2^{\mathrm{T}}(\theta)\mathbf{Q}(\xi)g(\xi)d\xi \qquad (107)
$$
$$
- \int_\theta^{2\pi} \mathbf{P}_2^{\mathrm{T}}(\theta)\mathbf{Q}(\xi)g(\xi)d\xi
$$
$$
= h_3(\theta),
$$

$$
\beta g(\theta) + \int_0^\theta \mathbf{P}_3^{\mathrm{T}}(\theta)\mathbf{Q}(\xi)f(\xi)d\xi
$$
$$
+ \int_\theta^{2\pi} \mathbf{P}_3^{\mathrm{T}}(\theta)\mathbf{Q}(\xi)f(\xi)d\xi
$$
$$
- \int_0^\theta \mathbf{P}_4^{\mathrm{T}}(\theta)\mathbf{Q}(\xi)g(\xi)d\xi \qquad (108)
$$
$$
- \int_\theta^{2\pi} \mathbf{P}_4^{\mathrm{T}}(\theta)\mathbf{Q}(\xi)g(\xi)d\xi
$$
$$
= h_4(\theta).
$$

Let us define

$$
\mathbf{u}_1(\theta) := \int_0^\theta \mathbf{Q}(\xi)f(\xi)d\xi, \qquad (109)
$$

$$
\mathbf{u}_2(\theta) := \int_{2\pi}^\theta \mathbf{Q}(\xi)f(\xi)d\xi, \qquad (110)
$$

$$
\mathbf{u}_3(\theta) := \int_0^\theta \mathbf{Q}(\xi)g(\xi)d\xi, \qquad (111)
$$

$$
\mathbf{u}_4(\theta) := \int_{2\pi}^\theta \mathbf{Q}(\xi)g(\xi)d\xi, \qquad (112)
$$

and Eqs. (107) and (108) can be expressed as

$$
\alpha f(\theta) + \mathbf{P}_1^{\mathrm{T}}(\theta)[\mathbf{u}_1(\theta) - \mathbf{u}_2(\theta)]
$$
$$
- \mathbf{P}_2^{\mathrm{T}}(\theta)[\mathbf{u}_3(\theta) - \mathbf{u}_4(\theta)] = h_3(\theta), \quad (113)
$$

$$
\beta g(\theta) + \mathbf{P}_3^{\mathrm{T}}(\theta)[\mathbf{u}_1(\theta) - \mathbf{u}_2(\theta)]
$$
$$
- \mathbf{P}_4^{\mathrm{T}}(\theta)[\mathbf{u}_3(\theta) - \mathbf{u}_4(\theta)] = h_4(\theta). \quad (114)
$$

Taking the differentials of Eqs. (109)-(112) with respect to θ we obtain

$$
\mathbf{u}_1'(\theta) = \mathbf{Q}(\theta)f(\theta), \qquad (115)
$$
$$
\mathbf{u}_2'(\theta) = \mathbf{Q}(\theta)f(\theta), \qquad (116)
$$
$$
\mathbf{u}_3'(\theta) = \mathbf{Q}(\theta)g(\theta), \qquad (117)
$$
$$
\mathbf{u}_4'(\theta) = \mathbf{Q}(\theta)g(\theta). \qquad (118)
$$

Inserting Eq. (113) for $f(\theta)$ and Eq. (114) for $g(\theta)$ into the above four equations we obtain

$$
\alpha \mathbf{u}_1'(\theta) = \mathbf{Q}\mathbf{P}_1^{\mathrm{T}}[\mathbf{u}_2(\theta) - \mathbf{u}_1(\theta)]
$$
$$
+ \mathbf{Q}\mathbf{P}_2^{\mathrm{T}}[\mathbf{u}_3(\theta) - \mathbf{u}_4(\theta)] + h_3(\theta)\mathbf{Q}, \quad \mathbf{u}_1(0) = \mathbf{0},
$$
$$
\tag{119}
$$

$$
\alpha \mathbf{u}_2'(\theta) = \mathbf{Q}\mathbf{P}_1^{\mathrm{T}}[\mathbf{u}_2(\theta) - \mathbf{u}_1(\theta)]
$$
$$
+ \mathbf{Q}\mathbf{P}_2^{\mathrm{T}}[\mathbf{u}_3(\theta) - \mathbf{u}_4(\theta)] + h_3(\theta)\mathbf{Q}, \quad \mathbf{u}_2(2\pi) = \mathbf{0},
$$
$$
\tag{120}
$$

$$
\beta \mathbf{u}_3'(\theta) = \mathbf{Q}\mathbf{P}_3^{\mathrm{T}}[\mathbf{u}_2(\theta) - \mathbf{u}_1(\theta)]
$$
$$
+ \mathbf{Q}\mathbf{P}_4^{\mathrm{T}}[\mathbf{u}_3(\theta) - \mathbf{u}_4(\theta)] + h_4(\theta)\mathbf{Q}, \quad \mathbf{u}_3(0) = \mathbf{0},
$$
$$
\tag{121}
$$

$$
\beta \mathbf{u}_4'(\theta) = \mathbf{Q}\mathbf{P}_3^{\mathrm{T}}[\mathbf{u}_2(\theta) - \mathbf{u}_1(\theta)]
$$
$$
+ \mathbf{Q}\mathbf{P}_4^{\mathrm{T}}[\mathbf{u}_3(\theta) - \mathbf{u}_4(\theta)] + h_4(\theta)\mathbf{Q}, \quad \mathbf{u}_4(2\pi) = \mathbf{0}.
$$
$$
\tag{122}
$$

The above four equations constitute two-point boundary value problems.

From Eqs. (115)-(118) it can be seen that $\mathbf{u}_1' = \mathbf{u}_2'$ and $\mathbf{u}_3' = \mathbf{u}_4'$, which mean that

$$
\mathbf{u}_1 = \mathbf{u}_2 + \mathbf{c}_1, \quad \mathbf{u}_3 = \mathbf{u}_4 + \mathbf{c}_2, \qquad (123)
$$

where $\mathbf{c}_1$ and $\mathbf{c}_2$ are constant vectors to be determined. By using the final conditions in Eqs. (120) and (122) we find that

$$
\mathbf{u}_1(2\pi) = \mathbf{u}_2(2\pi) + \mathbf{c}_1 = \mathbf{c}_1,
$$
$$
\mathbf{u}_3(2\pi) = \mathbf{u}_4(2\pi) + \mathbf{c}_2 = \mathbf{c}_2. \qquad (124)
$$

Substituting Eq. (123) into Eqs. (119) and (121) we have

$$
\alpha \mathbf{u}_1'(\theta) = -\mathbf{Q}(\theta)\mathbf{P}_1^{\mathrm{T}}(\theta)\mathbf{c}_1 + \mathbf{Q}(\theta)\mathbf{P}_2^{\mathrm{T}}(\theta)\mathbf{c}_2
$$
$$
+ h_3(\theta)\mathbf{Q}(\theta), \quad \mathbf{u}_1(0) = \mathbf{0}, \quad (125)
$$

$$\beta \mathbf{u}_3'(\theta) = -\mathbf{Q}(\theta)\mathbf{P}_3^{\mathrm{T}}(\theta)\mathbf{c}_1 + \mathbf{Q}(\theta)\mathbf{P}_4^{\mathrm{T}}(\theta)\mathbf{c}_2$$
$$+ h_4(\theta)\mathbf{Q}(\theta), \quad \mathbf{u}_3(0) = \mathbf{0}. \quad (126)$$

Integrating the above two equations and using the initial conditions it follows that

$$\mathbf{u}_1(\theta) = -\frac{1}{\alpha}\int_0^\theta \mathbf{Q}(\xi)\mathbf{P}_1^{\mathrm{T}}(\xi)d\xi\mathbf{c}_1$$
$$+ \frac{1}{\alpha}\int_0^\theta \mathbf{Q}(\xi)\mathbf{P}_2^{\mathrm{T}}(\xi)d\xi\mathbf{c}_2 \quad (127)$$
$$+ \frac{1}{\alpha}\int_0^\theta h_3(\xi)\mathbf{Q}(\xi)d\xi,$$

$$\mathbf{u}_3(\theta) = -\frac{1}{\beta}\int_0^\theta \mathbf{Q}(\xi)\mathbf{P}_3^{\mathrm{T}}(\xi)d\xi\mathbf{c}_1$$
$$+ \frac{1}{\beta}\int_0^\theta \mathbf{Q}(\xi)\mathbf{P}_4^{\mathrm{T}}(\xi)d\xi\mathbf{c}_2 \quad (128)$$
$$+ \frac{1}{\beta}\int_0^\theta h_4(\xi)\mathbf{Q}(\xi)d\xi.$$

Taking $\theta = 2\pi$ in the above equations and imposing the condition (124) one obtains the governing equations for $\mathbf{c}_1$ and $\mathbf{c}_2$:

$$\mathbf{R}_{11}\mathbf{c}_1 + \mathbf{R}_{12}\mathbf{c}_2 = \int_0^{2\pi} h_3(\xi)\mathbf{Q}(\xi)d\xi, \quad (129)$$

$$\mathbf{R}_{21}\mathbf{c}_1 + \mathbf{R}_{22}\mathbf{c}_2 = \int_0^{2\pi} h_4(\xi)\mathbf{Q}(\xi)d\xi, \quad (130)$$

where

$$\mathbf{R}_{11} := \alpha\mathbf{I}_{2m+1} + \int_0^{2\pi} \mathbf{Q}(\xi)\mathbf{P}_1^{\mathrm{T}}(\xi)d\xi, \quad (131)$$

$$\mathbf{R}_{12} := -\int_0^{2\pi} \mathbf{Q}(\xi)\mathbf{P}_2^{\mathrm{T}}(\xi)d\xi, \quad (132)$$

$$\mathbf{R}_{21} := \int_0^{2\pi} \mathbf{Q}(\xi)\mathbf{P}_3^{\mathrm{T}}(\xi)d\xi, \quad (133)$$

$$\mathbf{R}_{22} := \beta\mathbf{I}_{2m+1} - \int_0^{2\pi} \mathbf{Q}(\xi)\mathbf{P}_4^{\mathrm{T}}(\xi)d\xi. \quad (134)$$

Eqs. (129) and (130) can be used to determine $\mathbf{c}_1$ and $\mathbf{c}_2$ by considering

$$\begin{bmatrix} \mathbf{R}_{11} & \mathbf{R}_{12} \\ \mathbf{R}_{21} & \mathbf{R}_{22} \end{bmatrix}^{-1} = \begin{bmatrix} \mathbf{I}_{2m+1} & -\mathbf{R}_{11}^{-1}\mathbf{R}_{12} \\ \mathbf{0}_{2m+1} & \mathbf{I}_{2m+1} \end{bmatrix}$$
$$\cdot \begin{bmatrix} \mathbf{R}_{11}^{-1} & \mathbf{0}_{2m+1} \\ \mathbf{0}_{2m+1} & \mathbf{R}_0^{-1} \end{bmatrix} \begin{bmatrix} \mathbf{I}_{2m+1} & \mathbf{0}_{2m+1} \\ -\mathbf{R}_{21}\mathbf{R}_{11}^{-1} & \mathbf{I}_{2m+1} \end{bmatrix}$$
$$= \begin{bmatrix} \mathbf{R}_{11}^{-1} + \mathbf{R}_{11}^{-1}\mathbf{R}_{12}\mathbf{R}_0^{-1}\mathbf{R}_{21}\mathbf{R}_{11}^{-1} & -\mathbf{R}_{11}^{-1}\mathbf{R}_{12}\mathbf{R}_0^{-1} \\ -\mathbf{R}_0^{-1}\mathbf{R}_{21}\mathbf{R}_{11}^{-1} & \mathbf{R}_0^{-1} \end{bmatrix},$$
$$(135)$$

where

$$\mathbf{R}_0 = \mathbf{R}_{22} - \mathbf{R}_{21}\mathbf{R}_{11}^{-1}\mathbf{R}_{12}. \quad (136)$$

When $\mathbf{c}_1$ and $\mathbf{c}_2$ are available, from Eqs. (113), (114) and (123) we can calculate $f(\theta)$ and $g(\theta)$ by

$$\alpha f(\theta) = h_3(\theta) - \mathbf{P}_1(\theta)\cdot\mathbf{c}_1 + \mathbf{P}_2(\theta)\cdot\mathbf{c}_2, \quad (137)$$
$$\beta g(\theta) = h_4(\theta) - \mathbf{P}_3(\theta)\cdot\mathbf{c}_1 + \mathbf{P}_4(\theta)\cdot\mathbf{c}_2. \quad (138)$$

From Eqs. (124), (109) and (111) it follows that

$$\mathbf{c}_1 = \int_0^{2\pi} \mathbf{Q}(\xi)f(\xi)d\xi, \quad \mathbf{c}_2 = \int_0^{2\pi} \mathbf{Q}(\xi)g(\xi)d\xi. \quad (139)$$

Upon reminding Eq. (29) it can be understood that $\mathbf{c}_1$ is the vector composed of the Fourier coefficients of the unknown function $f(\theta)$, while $\mathbf{c}_2$ is the vector composed of the Fourier coefficients of the unknown function $g(\theta)$. Meanwhile, Eqs. (129) and (130) describe the relations between the Fourier coefficients of the boundary data on two artifical circles and the boundary data on the real boundaries. In terms of $\mathbf{c}_1$ and $\mathbf{c}_2$ we can write the solution directly,

$$u(r,\theta) =$$
$$\frac{1}{2}(a_0 + b_0\ln r) + \sum_{k=1}^m \Big[(a_k r^k + b_k r^{-k})\cos k\theta$$
$$+ (c_k r^k + d_k r^{-k})\sin k\theta\Big], \quad (140)$$

where

$$a_0 = \frac{1}{\pi(\ln r_1 - \ln r_2)}[c_1^1\ln r_1 - c_2^1\ln r_2], \quad (141)$$

$$b_0 = \frac{1}{\pi(\ln r_1 - \ln r_2)}[c_2^1 - c_1^1], \quad (142)$$

$$a_k = \frac{e_k c_2^{2k}}{r_2^k} - \frac{e_k c_1^{2k}}{r_1^k}, \quad (143)$$

$$b_k = e_k r_1^k c_1^{2k} - e_k r_2^k c_2^{2k}, \quad (144)$$

$$c_k = \frac{e_k c_2^{2k+1}}{r_2^k} - \frac{e_k c_1^{2k+1}}{r_1^k}, \quad (145)$$

$$d_k = e_k r_1^k c_1^{2k+1} - e_k r_2^k c_2^{2k+1}, \quad (146)$$

where c_1^k represents the k-th component of $\mathbf{c}_1$, while c_2^k represents the k-th component of $\mathbf{c}_2$.

10   The conjugate gradient method

In the above we have derived Eqs. (129) and (130) to calculate c_1 and c_2, and Eqs. (137) and (138) to calculate $f(\theta)$ and $g(\theta)$. An efficient numerical procedure can be derived as follows.

Let

$$\mathbf{R} := \begin{bmatrix} \mathbf{R}_{11} & \mathbf{R}_{12} \\ \mathbf{R}_{21} & \mathbf{R}_{22} \end{bmatrix}, \tag{147}$$

$$\mathbf{c} := \begin{bmatrix} \mathbf{c}_1 \\ \mathbf{c}_2 \end{bmatrix}, \tag{148}$$

$$\mathbf{b}_0 := \begin{bmatrix} \int_0^{2\pi} h_3(\xi)\mathbf{Q}(\xi)d\xi \\ \int_0^{2\pi} h_4(\xi)\mathbf{Q}(\xi)d\xi \end{bmatrix}, \tag{149}$$

and then Eqs. (129) and (130) can be written as

$$\mathbf{R}\mathbf{c} = \mathbf{b}_0. \tag{150}$$

Instead of Eq. (150) we consider the normal equation:

$$\mathbf{A}\mathbf{c} = \mathbf{b}, \tag{151}$$

where

$$\mathbf{A} := \mathbf{R}^\mathrm{T}\mathbf{R}, \tag{152}$$
$$\mathbf{b} := \mathbf{R}^\mathrm{T}\mathbf{b}_0. \tag{153}$$

Then, the conjugate gradient method as shown in Section 6 is applied on the above equation (151).

11   Numerical test II

11.1   Example 4

We consider a kite-shape outer boundary with the parameterization given by Eqs. (63) and (64). For the inner boundary we consider an apple-shape described by

$$r_4 = \frac{0.5 + 0.2\cos\theta + 0.1\sin 2\theta}{1.5 + 0.7\cos\theta}, \tag{154}$$
$$x_4(\theta) = r_4\cos\theta, \quad y_4(\theta) = r_4\sin\theta. \tag{155}$$

In order to test our method we consider an exact solution

$$u(r, \theta) = x^2 - y^2 = r^2\cos 2\theta, \tag{156}$$

which however led to rather complicated boundary conditions:

$$h_3(\theta) = u(r_3, \theta) = [(0.6\cos\theta + 0.3\cos 2\theta - 0.2)^2 + (0.6\sin\theta)^2]\cos 2\theta, \tag{157}$$

$$h_4(\theta) = u(r_4, \theta)$$
$$= \left(\frac{0.5 + 0.2\cos\theta + 0.1\sin 2\theta}{1.5 + 0.7\cos\theta} \right)^2 \cos 2\theta. \tag{158}$$

We solve $f(\theta)$ and $g(\theta)$ by the method in Section 10, whose results are shown in Figs. 6(a) and 6(b) under the parameters $r_1 = \max r_3 \approx 0.849$, $r_2 = \min r_4 \approx 0.257$, $m = 10$ and $\alpha = \beta = 10^{-8}$. Through 83 iterations with $\varepsilon = 10^{-15}$ the solution of $\mathbf{c}$ by Eq. (151) is obtained.
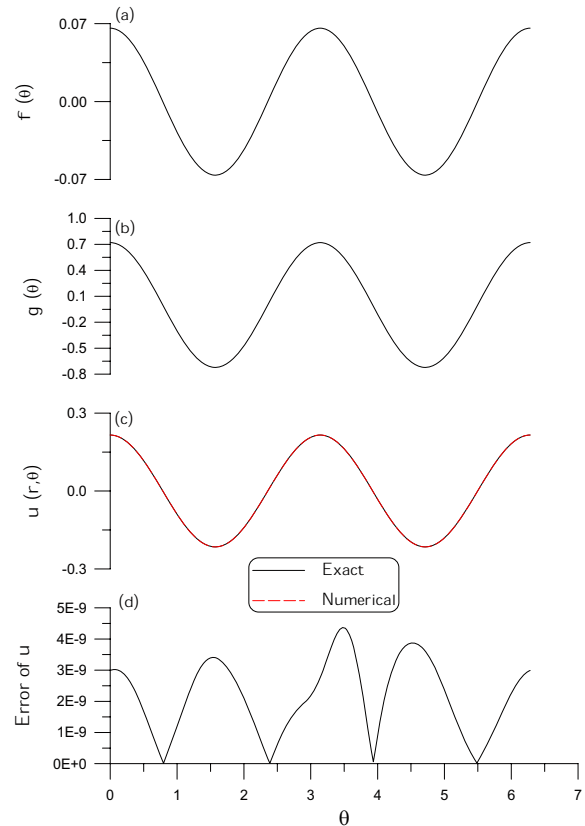
Figure 6: For Example 4: (a) plotting the function $f(\theta)$, (b) plotting the function $g(\theta)$, (c) comparing the numerical and exact solutions, and (d) plotting the numerical error of solution.

Then substituting **c** into Eqs. (140)-(146) we can obtain the numerical solution of u, of which a numerical solution along a circle with a radius $r = \max r_4$ was plotted in Fig. 6(c). The numerical error of u is shown in Fig. 6(d), which can be seen is smaller than 5×10^{-9}. It is a highly accurate numerical solution.

Next we replace the outer boundary by an epitrochoid boundary shape

$$r_3(\theta) = \sqrt{(a+b)^2 + 1 - 2(a+b)\cos(a\theta/b)},$$

(159)

$$x_3(\theta) = r_3 \cos\theta, \quad y_3(\theta) = r_3 \sin\theta \quad (160)$$

with $a = 4$ and $b = 1$. The inner boundary is four times large of the above kite. Under the parameters $r_1 = \max r_3 = 6$, $r_2 = \min r_4 \approx 1.028$, $m = 20$ and $\alpha = \beta = 10^{-8}$ we have calculated the numerical solution as compared with the exact solution $u = x^2 - y^2$ in Fig. 7(a) along a circle with a radius $r = \max r_4$. It can be seen that the new method leads to very accurate numerical result. Then, in Fig. 7(b) we compared the contour levels of potential $u = -6, -4, 2, 4$ for exact solutions and numerical solutions. It can be seen that the numerical results are almost coincident with the exact ones.

11.2 Example 5

We consider a kite-shape outer boundary as that used in the previous example but with its size being enlarged doubly. We consider the closed form solution

$$u(r, \theta) = e^x \cos y = e^{r\cos\theta} \cos(r\sin\theta). \quad (161)$$

The boundary conditions are very complicated for this example.

We apply the numerical method to this case under the parameters $r_1 = \max r_3 \approx 1.698$, $r_2 = \min r_4 \approx 0.257$, $m = 10$ and $\alpha = \beta = 10^{-8}$. Through 80 iterations the solution of **c** by Eq. (151) is obtained by subjecting to the criterion with $\varepsilon = 10^{-15}$. Then we can calculate $f(\theta)$ and $g(\theta)$ by Eqs. (137) and (138), whose results are shown in Figs. 8(a) and 8(b).
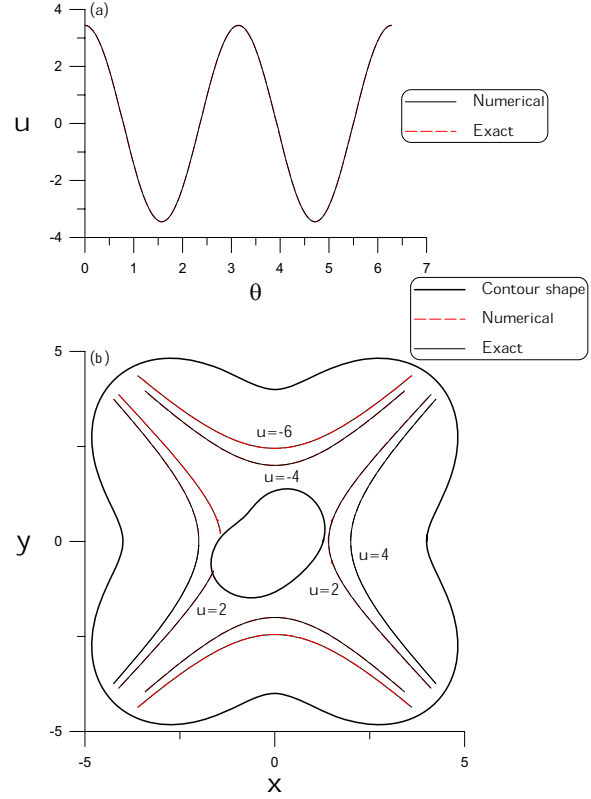
Figure 7: For Example 4 but with different boundaries: (a) comparing the numerical and exact solutions, and (b) comparing the numerical and exact contour levels of u.

Then, substituting **c** into Eqs. (140)-(146) we can obtain the numerical solution of u, of which a numerical solution along a circle with a radius $r = \max r_4$ was plotted in Fig. 8(c), which is close to the exact solution with the numerical error shown in Fig. 8(d). The numerical error of u is smaller than 3.5×10^{-8}.

12 Conclusions

In this paper we have proposed a new meshless method to calculate the solutions of Laplace equation in the arbitrary doubly-connected plane domains. It was demonstrated that in the regularized sense we can find the semi-analytical solutions of the boundary conditions on artificial circles, and thus by the Fourier series expansion we can calculate the solution at any point inside the domain.
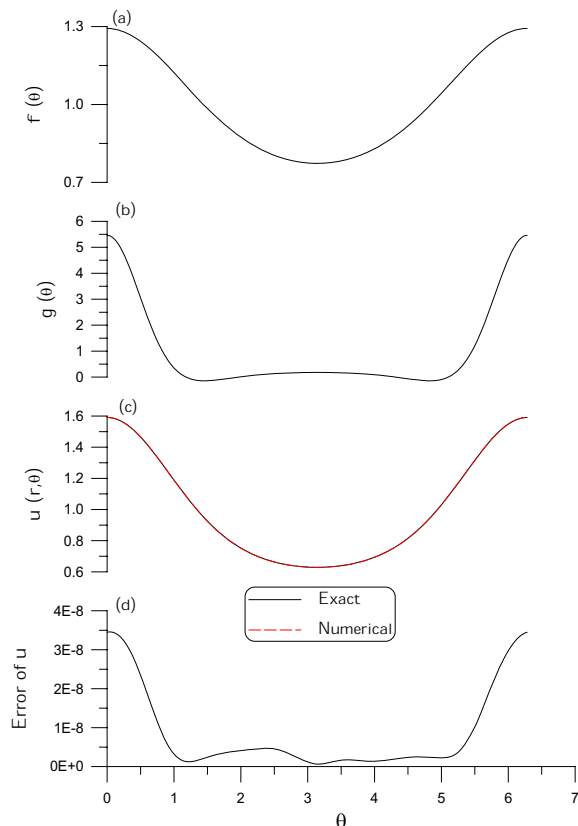
Figure 8: For Example 5: (a) plotting the function $f(\theta)$, (b) plotting the function $g(\theta)$, (c) comparing the numerical and exact solutions, and (d) plotting the numerical error of solution.

The numerical examples show that the effectiveness of the new method and the accuracy is rather good. The new method possesses several advantages than the conventional boundary-type solution methods, including mesh-free, singularity-free, non-illposedness, semi-analyticity of solution, efficiency, accuracy and stability.

References

Atluri, S. N.; Kim, H. G.; Cho, J. Y. (1999): A critical assessment of the truly meshless local Petrov-Galerkin (MLPG), and local boundary integral equation (LBIE) methods. *Computational Mechanics*, vol. 24, pp. 348-372.

Atluri, S. N.; Shen, S. (2002): The meshless local Petrov-Galerkin (MLPG) method: a simple & less-costly alternative to the finite element and boundary element methods. *CMES: Computer Modeling in Engineering & Sciences*, vol. 3, pp. 11-51.

Cao, Y.; Schultz, W.W.; Beck, R. F. (1991): Three-dimensional desingularized boundary integral methods for potential problems. *International Journal for Numerical Methods in Fluids*, vol. 12, pp. 785-803.

Chen, J. T.; Chang, M. H.; Chen, K. H.; Lin, S. R. (2002): The boundary collocation method with meshless concept for acoustic eigenanalysis of two-dimensional cavities using radial basis function. *Journal of Sound and Vibration*, vol. 257, pp. 667-711.

Chen, J. T.; Chang, M. H.; Chen, K. H.; Chen, I. L. (2002): Boundary collocation method for acoustic eigenanalysis of three-dimensional cavities using radial basis function. *Computational Mechanics*, vol. 29, pp. 392-408.

Chen, W.; Tanaka, M. (2002): A meshless, integration-free, and boundary-only RBF technique. *Computers and Mathematics with Applications*, vol. 43, pp. 379-391.

Chuang, J. M. (1999): Numerical studies on desingularized Cauchy's formula with applications to interior potential problems. *International Journal for Numerical Methods in Engineering*, vol. 46, pp. 805-824.

Fairweather, G.; Karageorghis, A. (1998): The method of fundamental solutions for elliptic boundary value problems. *Advances in Computational Mathematics*, vol. 9, pp. 69-95.

Fan, C. M.; Young, D. L. (2002): Analysis of the 2D Stokes flows by the nonsingular boundary integral equation method. *International Mathematical Journal*, vol. 2, pp. 1199-1215.

Golberg, M. A.; Chen, C. S. (1996): Discrete Projection Methods for Integral Equations. Computational Mechanics Publications, Southampton.

Huang, S. C.; Shaw, R. P. (1995): The Trefftz method as an integral equation. *Advances in Engineering Software*, vol. 24, pp. 57-63.

Hwang, W. S.; Huang, Y. Y. (1998): Nonsingular direct formulation of boundary integral equations for potential flows. *International Journal for*

Numerical Methods in Fluids, vol. 26, pp. 627-635.

Jin, B.; Chen, W. (2006): Boundary knot method based on geodesic distance for anisotropic problems. *Journal of Computational Physics*, vol. 215, pp. 614-629.

Kita, E.; Kamiya, N. (1995): Trefftz method: an overview. *Advances in Engineering Software*, vol. 24, pp. 3-12.

Kress, R. (1999): Linear Integral Equations. 2nd ed., Springer, Berlin.

Lalli, F. (1991): On the accuracy of the desingularized boundary integral method in free surface flow problems. *International Journal for Numerical Methods in Fluids*, vol. 25, pp. 1163-1184.

Landweber, L.; Macagno, M. (1969): Irrotational flow about ship forms. IIHR Report No. 123, Iowa University.

Lavrentiev, M. M. (1967): Some Improperly Posed Problems of Mathematical Physics. Springer, New York.

Liu, C.-S. (2001): Cone of non-linear dynamical system and group preserving schemes. *International Journal of Non-Linear Mechanics*, vol. 36, pp. 1047-1068.

Liu, C.-S. (2005): Nonstandard group-preserving schemes for very stiff ordinary differential equations. *CMES: Computer Modeling in Engineering & Sciences*, vol. 9, pp. 255-272.

Liu, C.-S. (2007a): Elastic torsion bar with arbitrary cross-section using the Fredholm integral equations. *CMC: Computers, Materials & Continua*, vol. 5, pp. 31-42.

Liu, C.-S. (2007b): A highly accurate collocation Trefftz method for solving the Laplace equation in the doubly connected domains. *Numerical Methods for Partial Differential Equations*, in press, 2007.

Saavedra, I.; Power, H. (2003): Multipole fast algorithm for the least-squares approach of the method of fundamental solutions for three-dimensional harmonic problems. *Numerical Methods for Partial Differential Equations*, vol. 19, pp. 828-845.

Young, D. L.; Chen, K. H.; Lee, C. W. (2005): Novel meshless method for solving the potential problems with arbitrary domain. *Journal of Computational Physics*, vol. 209, pp. 290-321.

Young, D. L.; Hwang, W. S.; Tsai, C. C.; Lu, H. L. (2005): Accuracy of desingularized boundary integral equations for plane exterior potential problems. *Engineering Analysis with Boundary Elements*, vol. 29, pp. 224-231.

Young, S. A. (1999): A solution method for two-dimensional potential flow about bodies with smooth surfaces by direct use of the boundary integral equation. *Communications in Numerical Methods in Engineering*, vol. 15, pp. 469-478.

Zhang, Y. L.; Yeo, K. S.; Khoo, B. C.; Chong, W. K. (1999): Simulation of three-dimensional bubbles using desingularized boundary integral method. *International Journal for Numerical Methods in Fluids*, vol. 31, pp. 1311-1320.